









Exceptional preservation of three-dimensional dunes on an ancient deep-marine seafloor: implications for sedimentary processes and depositional environments

Euan L. Soutter^{1*}, Ander Martínez-Doñate^{1,2} , Ian A. Kane¹ , Miquel Poyatos-Moré³ , William J. Taylor⁴ , David M. Hodgson⁴ , Max J. Bouwmeester¹ , Stephen S. Flint¹

¹ Department of Earth and Environmental Sciences, University of Manchester, Manchester M13 9PL, UK

² Bureau of Economic Geology, Jackson School of Geosciences, The University of Texas at Austin, Austin, Texas

³ Departament de Geologia, Universitat Autònoma de Barcelona, 08193 Cerdanyola del Vallès, Spain

⁴ Stratigraphy Group, School of Earth and Environment, University of Leeds, Leeds, LS2 9JT

*corresponding author: Euan L. Soutter (euan-soutter@hotmail.co.uk)

doi:10.57035/journals/sdk.2024.e21.1067

Editors: Victoria Valdez Buso, Anna Pontén and Julien Bailleul

Reviewers: Allard Martinius and Richard Wild

Copyediting, layout and production: Romain Vaucher, Madeleine Vickers and Gabriel Bertolini

Submitted: 20.01.2023

Accepted: 22.11.2023

Published: 10.01.2024

Abstract | Depositional and erosional bedforms can be used to reconstruct sedimentary processes and aid palaeoenvironmental interpretations. Using exhumed deep-marine strata in the Eocene Aínsa Basin, Spain, we document a 3-dimensional package of dunes, a rarely identified bedform in deep-marine environments. Our analysis shows that the dunes have curvilinear crests in planform, with smaller superimposed oblique dunes and ripples across the stoss sides. Beds containing these dunes have two main internal divisions: a lower inversely-graded (fine-to-coarse sandstone) and predominantly structureless division, and an upper coarse-grained sandstone division with well-developed cross-stratification, which is scoured and mantled with mudclasts and coarse-grains on the stoss-side. The rugose remnant relief of the bedforms controls the location of subsequent bedforms. Following recently reported direct measurements of natural turbidity currents, we interpret the basal division as recording deposition from the dense basal head of a high-velocity turbidity current, followed by the development of dunes beneath the more sustained but relatively high-velocity and unsteady flow body that reworked the initial sandy deposit into downstream migrating dunes and scours. These dune-forming beds have been identified in different deep-water environments in the Aínsa Basin stratigraphy, including channel overbank and channel mouth settings and scour-fills. These locations suggest that the dunes were intimately tied to high-velocity flows that bypassed through channel axes before expanding and depositing in less confined channel overbank or channel mouth settings. Preservation of these dunes in the Aínsa Basin was likely enhanced by tectonically-forced lateral migration of channels, which prevented cannibalisation of bypass-dominated zones, in combination with high aggradation rates due to confinement. Where identified these dune-like bedforms are considered diagnostic of substantial sediment bypass downslope to deep-water basins.

Lay summary | Sediment on the Earth's surface or at the bottom of the sea is built into different structures by wind and water currents, forming bedforms related to the properties of these currents. In deep marine environments, turbulent mixtures of sediment and water (turbidity currents) flowing along the seabed can create bedforms that may be preserved in the geological record. Bedforms called dunes, which are commonly formed by wind and rivers, are rarely formed by turbidity currents. When dunes are observed in turbidity current deposits, it is therefore important to study them. Using a rare three-dimensional exposure of deep-marine dunes in the Eocene Aínsa Basin of the Pyrenean foreland, Spain, we explore the formation of dunes beneath turbidity currents. The studied dunes are associated with both erosion of the seabed and coarse-grained deposition, indicating they were deposited by powerful and sustained turbidity currents. Since these types of currents are commonly associated with submarine channels and channel-mouths, this indicates that dunes may be commonly formed in channelised deep-marine environments. Their lack of preservation in the geological record may be partially attributed to the erosive environments in which they form, with dunes having a high likelihood of being eroded as channels move around the seabed.

Keywords: Dunes, deep-marine, Pyrenees, Aínsa, turbidite

1. Introduction

Fluidal flows can deposit and entrain sediment as they flow over a moveable bed, forming a suite of erosional and depositional bedforms related to the properties of both the fluid and the bed. Since different sedimentary environments are associated with different prevailing flow conditions, assemblages of bedforms can be used to reconstruct palaeoenvironments from the sedimentary record (e.g., Allen, 1982; Southard & Boguchwal, 1990; Reading, 2009; Collinson & Mountney, 2019). Further study on the distribution of bedforms in sedimentary systems and the conditions under which various bedforms develop is therefore critical for improving the accuracy of palaeohydraulic and palaeoenvironmental reconstructions (e.g., Leeder, 1983; Dumas et al., 2005). In deep-water settings, bedforms are typically formed by turbidity currents, which are turbulent mixtures of sediment and water that flow downslope due to their excess density (e.g., Kuenen & Migliorini, 1950; Sequeiros et al., 2010; Meiburg & Kneller, 2010), or by more dilute density currents, such as contour currents, where excess density is a consequence of temperature and/or salinity gradients in the ocean (e.g., Rodrigues et al., 2022). A wide variety of bedforms can form beneath these currents (e.g., Fedele et al., 2016; Cartigny & Postma, 2017), and they are commonly used to aid reconstructions of deep-water processes and environments in modern (e.g., Hage et al., 2018; Normandeau et al., 2020) and ancient (e.g., Komar, 1991; Baker & Baas, 2020) sedimentary systems.

Dunes, which migrate downstream by erosion of an upstream-facing stoss-side and deposition on a downstream-facing lee-side, should precede ripples in the stratigraphic record of an 'ideal' decelerating sandy turbidity current (Bouma, 1962; Tilston et al., 2015), and therefore be relatively common in turbidity current deposits, known as 'turbidites'. The transition from ripples to dunes can be defined hydrodynamically, as the point at which the bedform is in phase with the upper surface of the lower layer of a turbidity current (e.g., Fedele et al., 2016; de Cala et al., 2020), or based on dimensions (particularly in ancient deposits), with dunes tending to be larger and spaced more widely (e.g., Ashley, 1990). While ripples are commonly identified in turbidites, deep-water dunes are rarely identified, which has attracted interest for decades (e.g., Walton, 1967; Arnott, 2012). The relative paucity of dunes compared to other bedforms in turbidites has been attributed to: 1) turbulent flows having deposited their coarse grains prior to entering the dune-forming velocity and grain size phase (Walton, 1967), 2) high flow densities and sedimentation rates in the dune-forming velocity phase suppressing dune formation (Lowe, 1988; Arnott, 2012), 3) a lack of time spent in the dune-forming phase (Walker, 1965; Pickering & Hiscott, 1991), 4) high clay contents altering the flow and/or bed rheology (Simons et al., 1963; Baas & Best, 2002; Schindler et al., 2015), and 5) the narrow grain size range capable of generating steep enough density gradients to create the angular bed

defects required for dune development (Tilston et al., 2015). Low preservation potential may also be an issue, with the high-velocity flows necessary for dune formation likely associated with net-erosional environments, such as channels (e.g., Conway et al., 2012). Dunes are therefore only sporadically identified in exhumed deep-water sedimentary basins when compared with other bedforms and other sedimentary environments (e.g., Bouma, 1962; Ricci Lucchi & Valmori, 1980; Pickering & Hiscott, 1991; Amy et al., 2000; Kneller & McCaffrey, 2003; Sumner et al., 2012; Stevenson et al., 2015). Consequently, the conditions required for dune formation and preservation, their internal structure, and their palaeogeographic significance in deep-water environments remain relatively weakly constrained.

Here, we document an example of sandstone dunes within the deep-marine Eocene Aínsa depocentre, south Pyrenean foreland basin (Figure 1), in which excellent exposure allows for detailed descriptions and quantification of dune-field morphology and internal characteristics. We aim to collate previous studies that have documented and discussed dunes of this style elsewhere in the Aínsa depocentre (Mutti & Normark, 1987; Mutti, 1991; Bakke et al., 2008; Cornard & Pickering, 2019; Tek et al., 2020), by discussing the origin, processes and palaeogeographic significance of these packages explicitly, and in light of direct measurements of modern turbidity currents.

2. The Aínsa depocentre and the Banastón system

The Aínsa depocentre is interpreted to represent the submarine slope segment (during the lower to middle Eocene) of the SE-NW trending south Pyrenean foreland basin and has been the subject of decades of research (Figure 1A) (e.g., van Lunsen, 1970; Puigdefàbregas & Souquet, 1986; Mutti, 1991; Pickering & Bayliss, 2009; Fernández et al., 2012; Mochales et al., 2012; Castelltort et al., 2017; Cantalejo et al., 2021a, b). Seven different sandstone-rich turbidite systems have been mapped within the basin-fill, each related to either tectonic uplift in the hinterland and subsidence in the depocentres and/or climatic and glacio-eustatic fluctuations (e.g., Pickering & Bayliss, 2009; Castelltort et al., 2017; Cantalejo et al., 2021a; Lächli et al., 2021).

This study focuses on the Banastón system, which was deposited over ~2 Myr during the Lutetian (Cantalejo et al., 2021b) and is interpreted as a series of channel-levée-overbank complexes that reach a thickness of 700 m on the lower slope (Bayliss & Pickering, 2015). In particular, we focus on Banastón II, a sand-rich unit within the larger Banastón system that was topographically steered through the NW-trending basin by syn-depositional deformation of NE and SW laterally confining basin margins and mass-transport deposits (Figure 1B) (Pickering & Bayliss, 2015; Martínez-Doñate et al., 2023). The package of interest is interpreted to represent the overbank of a channel confined by an actively-deforming

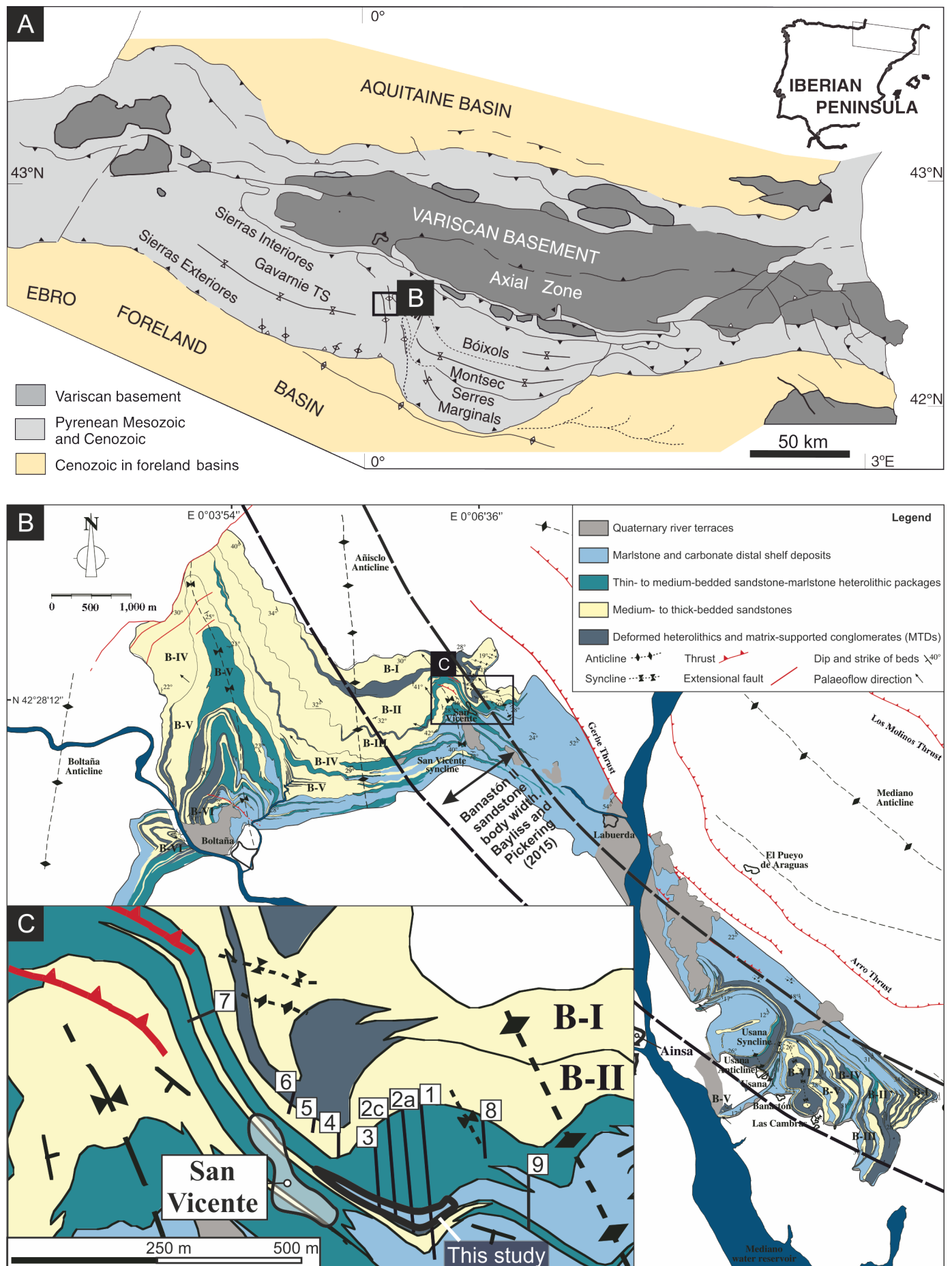


Figure 1 | (A) Geological map of the Pyrenees. This study focuses on the Cenozoic part of the foreland basin fill. TS; thrust sheets. (B) Geological map of the deep-marine Banastón system within the Cenozoic Aínsa depocentre (modified from Bayliss & Pickering 2015). This study concentrates on an interval within Banastón II (modified from Martínez-Doñate et al., 2023). B; Banastón. Measured sections indicated by numbers. Structural key in B applies in greyscale to A. (C) Geological map of the study area (modified from Pickering & Bayliss, 2009; Bayliss & Pickering, 2015; Martínez-Doñate et al., 2023). The basin had a ramp-like structure, therefore the boundary between the distal shelf and slope was likely gradual, hence the coincidence of deep-marine submarine channels and distal shelf deposits.

basin margin (Martínez-Doñate et al., 2023). This contrasts with most channels described in the literature in that the overbank is directly connected to the channel axis.

3. Methods

The locality lies ~270 m east of San Vicente (42.4675°, 0.111944°) and forms part of the study by Martínez-Doñate et al. (2023), who investigated the larger-scale evolution of the Banastón II system in this region (Figure 1C and 2). This study focuses on the detailed characterisation of a specific part of this succession using additional data. For a detailed stratigraphic, palaeogeographic and facies analysis see Martínez-Doñate et al. (2023).

Eight sections (26 m cumulative) from the deposits of interest within the succession were measured at a 1:5 scale to capture centimetre-scale sedimentary features and were correlated by walking individual beds and Uncrewed Aerial Vehicle (UAV) photogrammetry to capture thickness and sedimentary facies variations (Figures 3, 4 and 5) (see Martínez-Doñate et al., 2023 for UAV mapping of the interval). Bedform orientation measurements (n = 244) were collected through the downstream axes of seven dunes exposed on a bedding plane (Figure 6). The morphology of part of the dune-field was also measured using LiDAR (laser imaging, detection, and ranging) (Figure 7).

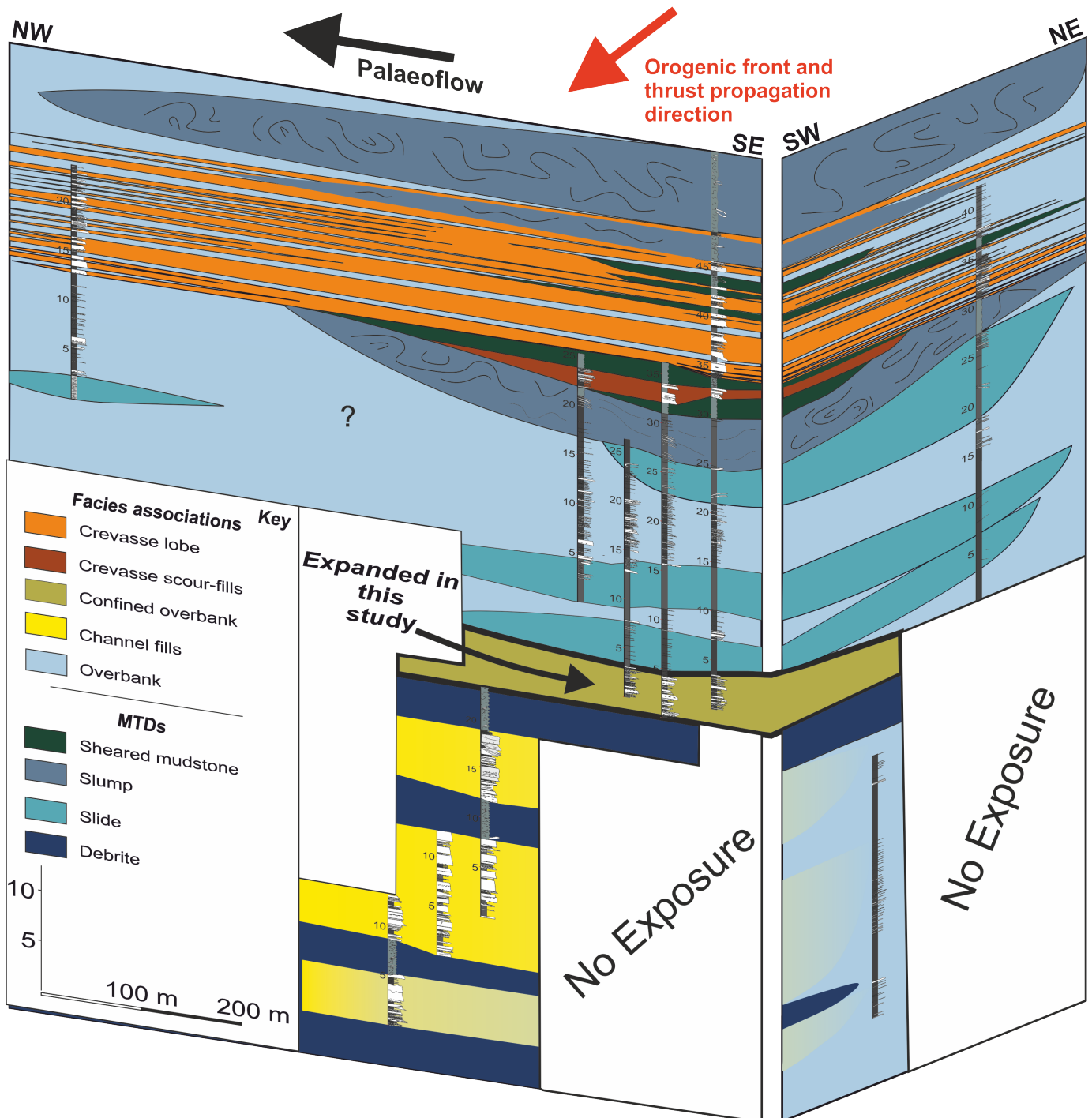


Figure 2 | Correlation panel showing the depositional elements and stratigraphic evolution of the Banastón II system (modified from Martínez-Doñate et al., 2023). The interval of interest is highlighted in black and is interpreted as the confined overbank of an adjacent channel to the ~SW. See Figure 1C for location.

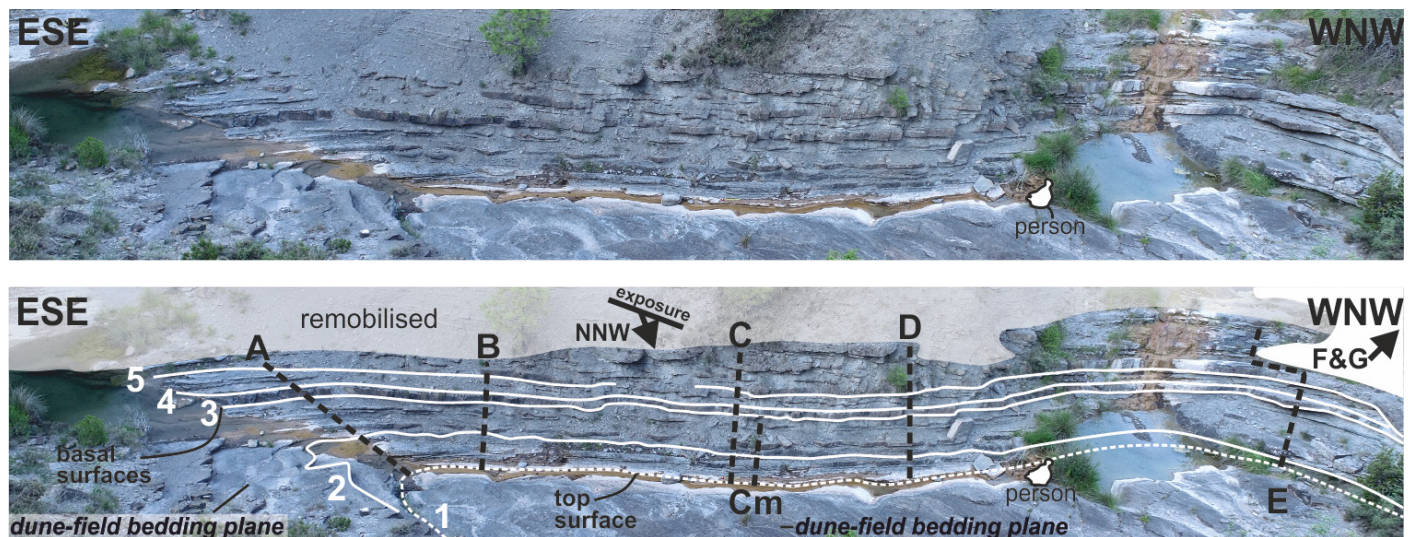


Figure 3 | The interval of interest and the measured sections used to describe the sedimentology of the interval. A person is sitting on a well-exposed dune-field, which has the same facies as the cross-stratified beds within the measured sections. Numbers and horizontal white lines refer to key marker beds in Figure 4.

Measurements at 5 cm intervals along these bedding planes allowed seven dune axis profiles to be calculated via trigonometry. Axial planes through each dune were used to reconstruct the dominant migration direction. Palaeocurrents were observed and collected from sole marks (flutes and grooves), ripple and dune foresets in the predominantly the thicker-beds (> 10 cm) within the interval of interest ($n = 47$) (Figure 4). Five samples were collected at regular intervals through a representative bed with coarse-grained dunes. Petrographic analysis (point-counting of 200 points per sample) allowed vertical grain size and sorting trends to be assessed.

4. Results

4.1. Palaeocurrents

Sole-mark and foreset orientations are dominantly oriented toward the NW and NNW, consistent with palaeoflow measured throughout the Banastón system (Bayliss & Pickering, 2015) and the deep-marine Aínsa Basin more broadly (e.g., Pickering & Bayliss, 2009) (Figures 4 and 6). The section is therefore oriented oblique-perpendicular to palaeoflow (flow out of section toward viewer). Dunes superimposed on larger dunes show divergence from this pattern, with foresets trending toward the NE and SW (Figure 6). Ripples also show some divergence from the sole marks, being dominantly oriented to the NW and sometimes showing complete reversal toward the SE (Figure 4). No upslope-accreting bedforms were observed.

4.2. Sedimentary facies

The typical vertical sequence of the dune-forming beds begins with an erosion surface that cuts into the underlying fine-grained substrate, overlain by a structureless or faintly planar-laminated basal division (Figures 4, 5 and 8). This division may pass vertically into a mud- and lithoclast-rich division across an amalgamation surface that is more heavily weathered when dominated by mud-clasts

and better preserved when dominated by lithoclasts or may be immediately overlain by coarse-grained foresets (Figure 8), often with abundant Nummulites. The lithoclasts are extra-basinal (Caja et al., 2010) and derived from the hinterland. Where the clast-rich division is present, the overlying foresets downlap and taper out within it. These foresets are commonly overlain by a fine-grained, ripple-laminated division, which infills depositional relief present on the foreset bedform and forms a grain-size break with the underlying coarse-grained foresets. Fine-grained intervals and other abrupt grain-size breaks are not observed in the foresets, supporting deposition under a single event. The bed tops are heavily bioturbated by horizontal, tube-like burrows that branch at approximately 90°, identified as *Thalassinoides*. Bed tops are commonly marked by patches of coarse grains and small mud clasts (< 2 cm), which mantle spoon-shaped scour surfaces. These beds also have a distinct reddish colour compared to beds within the underlying and overlying packages (Martínez-Doñate et al., 2023).

Laterally, these beds show substantial textural (granule to medium-grained) and thickness (10 to 25 cm) variation over tens of centimetres, with divisions composed of prominent foresets passing into faintly cross-bedded or structureless divisions (Figure 4). Shorter-wavelength thickness variation is also accommodated by relief present on the foresets (Figure 8), with overlying beds thickening where foresets in the underlying bed taper out. On a more regional scale, these packages show an overall thinning trend toward the NE, consistent with thinning of the Banastón II as a whole toward a NE-confining intrabasinal slope (Figure 2) (Bayliss & Pickering, 2015; Martínez-Doñate et al., 2023).

Thin-bedded (< 0.1 m) and normally-graded (silt-to-fine-grained sand) beds occur between these coarse-grained beds, along with fine-grained mass-transport deposits that contain deformed thin-beds (see Martínez-Doñate et al., 2023 for full description).

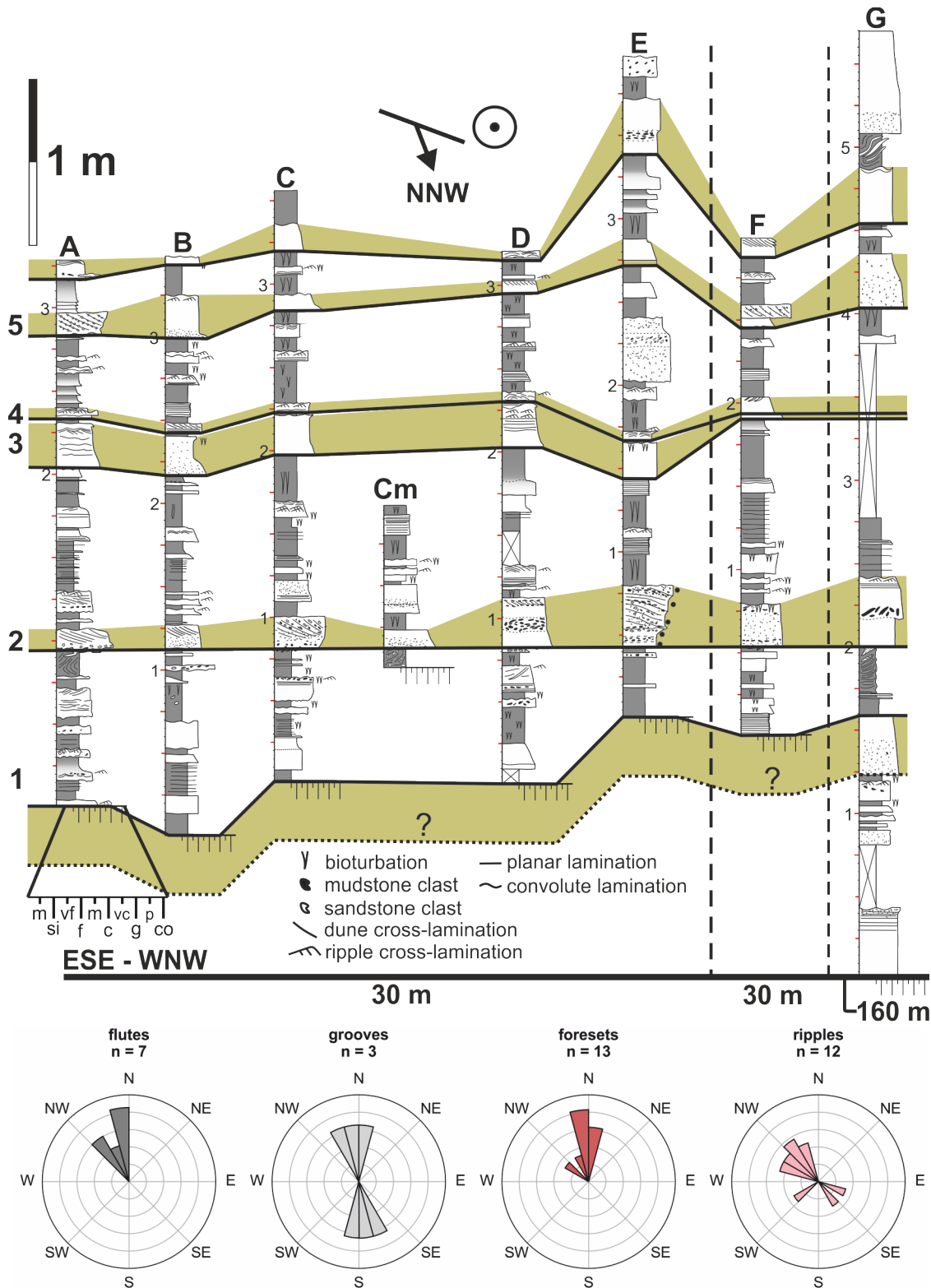


Figure 4 | Measured sections from Figures 2 & 3 (same datum), and palaeocurrent rose diagrams. Coarse-grained, cross-stratified marker beds are highlighted in green. Foreset measurements from dunes and superimposed dunes preserved on the key bedding plane are analysed separately (Figure 6). See Figure 1C for location.

4.3. Petrography

Point-counting indicates that the basal divisions of these beds are strongly inversely-graded, with median grain sizes passing from fine to coarse sand through the basal 5 cm (Figure 9). The fine-grained sandstone base of this division also spans a much narrower grain size range than the coarse-grained top, which contains grain sizes from silt- to granule (Figure 9). Samples from the foresets overlying this division are similarly coarse-grained with a

wide grain size range (Figure 9). Point-counting indicates little vertical variation in median grain size within the foresets when compared to the base of the bed, with visual measurements showing a weak inverse-grading from coarse to very coarse sand. Across the samples, sorting values fall between 0.8 and 1 Φ , indicating moderate sorting throughout the bed (Blair & McPherson, 1999).

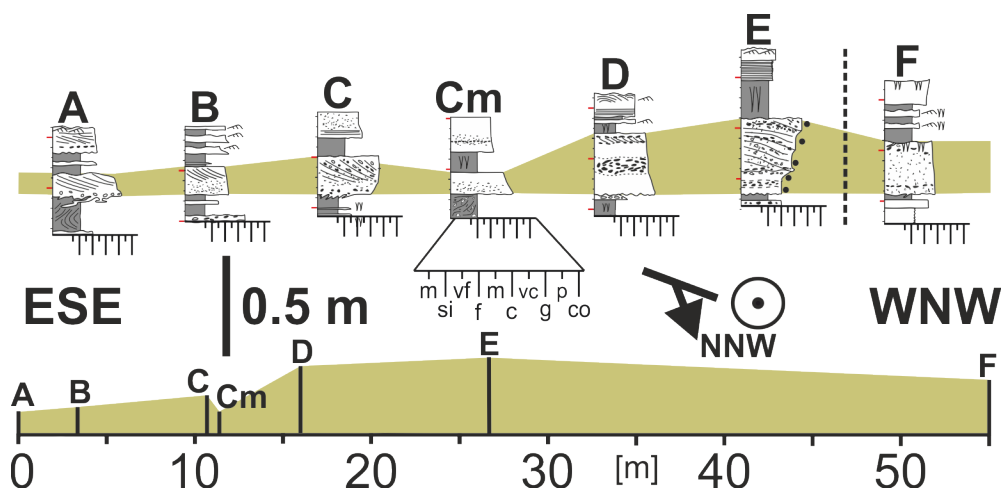


Figure 5 | Sedimentology of key marker bed 2 (Figure 4) with well-developed dunes (upper) and its true (x-axis-scaled) horizontal thickness variation (lower).

4.4. Dune morphology

The dunes have a wavelength (crest to next downstream crest along the axis of migration) of 1.5 to 2 m, with the distance between the crest and the trough varying between 0.5 m to 1 m (Figure 6). Crest heights (relative to the trough) range between 0.05 - 0.1 m. Restored dune gradients are horizontal to 5° on stoss-slopes and up to 10° on lee-slopes. These (compacted) lee gradients are consistent with dunes formed by major rivers in the present, with 75% of fluvial dunes having lee-slopes of < 14.9° (Cisneros et al., 2020); however, migration of superimposed dunes, scouring, compaction and the inherent difficulty in restoring bedforms from tectonically-tilted surfaces will all have modified the measured lee-slope bedforms, making 'true' values for depositional heights and gradients difficult to assess (Figure 8A).

Spoon-shaped metre-wide scour surfaces are cut into the lee slope, and are mantled by mud clasts and coarse-grained sand lags. These surfaces shallow and widen downdip, with dunes inset into these erosion surfaces, with stoss-sides tending to have a lower elevation than stoss-sides immediately upslope, indicating coupled erosion and deposition during dune migration under unsteady flows.

In planform view, the dunes have arcuate shapes and resemble barchan or lunate dunes commonly described in aeolian (e.g., Tsoar, 2001), shelfal (e.g., Todd, 2005), and, more rarely, in deep-marine settings, where they tend to be larger (10s to 100s of metres), finer-grained and formed by contour currents (e.g., Kenyon et al., 2002; Wynn et al., 2002; Miramontes et al., 2019) (Figure 6). This shape appears to be partially the result of scouring. Dune widths (from downstream crest tip to downstream crest tip across depositional-strike) range from 2 - 0.5 m. Superimposed dunes on the stoss-side are finer-grained and straight-crested (crest perpendicular to flow direction) (Figure 6A). Ripples on the dune surface tend to be lunate in planform, as imaged on the stoss-side of barchan dunes on the present-day seafloor (Wynn et al., 2002).

5. Discussion

5.1. Flow processes

The deposition of a structureless, inversely-graded, and poorly-sorted division supports the initial passage of a high concentration flow (e.g., Lowe, 1982), which may have been deposited above a bedform with a longer wavelength than can be constrained at the outcrop. Inverse-grading likely reflects kinematic sieving and squeezing within the highly-concentrated basal layer, with fine grains 'sieved' downwards between coarse grains, and coarse grains 'squeezed' upwards by friction during transport (Le Roux, 2003). Inverse-grading can also be caused by coarse grains being transported more slowly than fine grains (e.g., Hand, 1997), or flow waxing, such as when flows are sourced directly by rivers (e.g., Mulder et al., 2001). Contemporaneous deposition of both low-density mud clasts and higher-density lithoclasts, along with a predominantly structureless sandy layer, indicates high rates of deposition and inhibited sorting, possibly due to flow capacity loss.

Reworking of this sandy layer into down-stream migrating dunes indicates that the flow evolved towards lower velocities and concentrations with reduced rates of deposition, but still maintained high enough velocity and shear stress to form dunes. Direct measurements of turbidity currents indicate that this flow phase could have persisted over a relatively long time period (several hours to days), potentially encouraging the formation of dunes (Figure 10). An alternative explanation may be that the flow was pulsed, or a separate and subsequent lower-concentration flow reworked the initial deposit; however the lack of a break between the basal division and the dune-prone division supports the passage of one flow.

Dune formation may have been promoted by the initial deposition of the sandy layer, as dune formation requires a substrate with a low clay content (Schindler et al., 2015). The presence of grain flow deposits and scouring at the foot of the lee-slope indicates flow separation at the

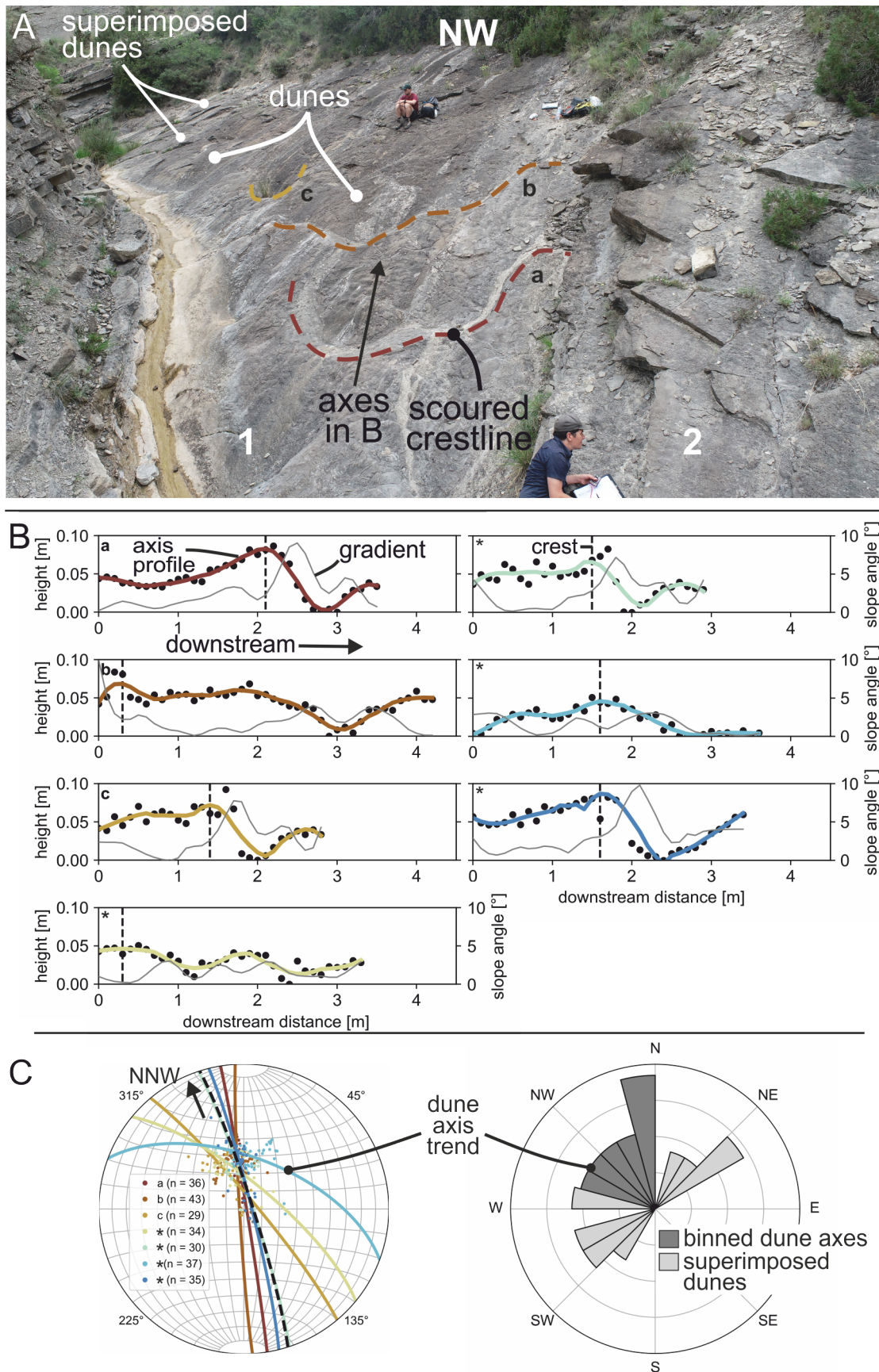


Figure 6 | (A) Bedding plane with curvilinear dunes and spoon-shaped scours. Exposure in Figure 3 to the left. (B) Downstream dune morphologies and gradients. Location of dune crestlines a, b and c in A. Asterisk (*) indicates dune profile unclear in A due to perspective. C. Dune axis trends and associated rose diagram. Dunes predominantly migrate to the NNW, while superimposed dunes migrate toward the SW and NE.

bedform crest, supporting the interpretation of downstream migration (e.g., Sequeiros et al., 2010). Supercritical bedforms, such as antidunes, may have preceded the dunes; however, they will have been reworked into dunes

and are, therefore, not preserved (de Cala et al., 2020). Downstream-migrating dunes may form beneath supercritical flows (Fedele et al., 2016), precluding any estimates

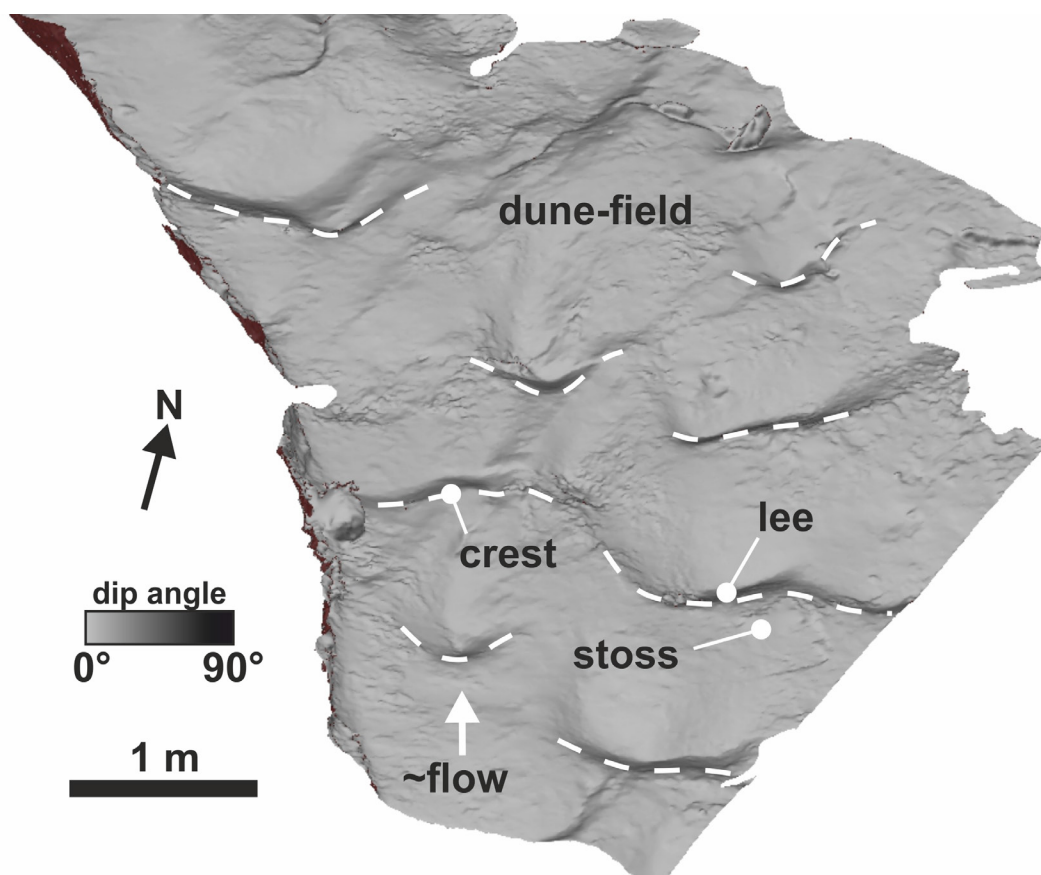


Figure 7 | Lidar scan of part of the dune-field (Figure 6A) coloured by dip-angle. Note steep downstream dipping lee-sides and shallow upstream-dipping stoss-sides. The sinuous shape of the dune crests and their tendency to merge along strike is also apparent.

of flow criticality based on the presence of down-stream migrating dunes alone.

The presence of finer-grained dunes and ripples superimposed on the larger, primary dunes indicates further waning of the flow, resulting in the deposition of smaller, finer-grained bedforms. Divergence of the superimposed dune migration directions from the primary dune migration direction suggests that the waning flow was increasingly deflected across the stoss side of the primary dunes, as observed in deep-marine barchan dunes (Wynn et al., 2002). Flow deflection may also have been enhanced by local mass-transport-related relief or regional tectonic topography (e.g., Soutter et al., 2021), which have been interpreted to strongly influence depositional processes in this area (Martínez-Doñate et al., 2023) (Figure 10). The superimposed dunes also have more linear crestlines than the underlying larger dunes, which is likely a consequence of reduced scouring and reworking on the stoss-sides of the smaller dunes, and/or linear crestlines tending to be more stable at lower flow velocities (Costello & Southard, 1981). The final stage of flow evolution is represented by the upper fine-grained/silt division, which we interpret as deposited by the low-velocity tail of the flow, with shear stresses such that silt can settle, followed by ambient seawater conditions (Figure 10). Differentiating the transition from turbiditic to hemipelagic deposition is difficult at the outcrop, with apparently hemipelagic deposits observed to comprise mm-thick turbidites in other deep-marine successions (Boulesteix et al., 2019).

Spatially, these beds show tens of centimetres of vertical thickness variation over tens of centimetres laterally. Internal structures also vary spatially, transitioning from structureless to convolute laminated beds with multiple amalgamation surfaces and grain-size breaks (Figures 4 and 5). This abrupt variation in thickness and facies is likely a consequence of autogenic velocity fluctuations of the highly-energetic flows that deposited them, causing frequent transitions through the depositional and erosional boundary, both spatially and temporally (e.g., Ge et al., 2022).

Dune preservation is therefore limited to: 1) high-magnitude flows that are capable of sustaining high enough velocities to build dunes following deposition of their coarse load (e.g., Sylvester & Lowe, 2004), 2) flows with a coarse enough load to occupy the dune-building phase (e.g., Fedele et al., 2016), and 3) flows traversing a sandy substrate with little cohesive clay (Schindler et al., 2015). The lack of clay or fine silt could also reflect flows originating from sand-rich sources; however, this option needs to be tested through a detailed study linking facies with provenance across the basin-fill. Assuming an approximately normal grain size distribution, these beds indicate major sediment bypass downslope, as finer-grained suspended sediment was continuously bypassed downstream during dune migration. The grain-size break between the coarse-grained dunes below and fine-grained ripples above supports this, with the missing grain-size fraction likely bypassed downslope (e.g., Stevenson et al., 2015), where

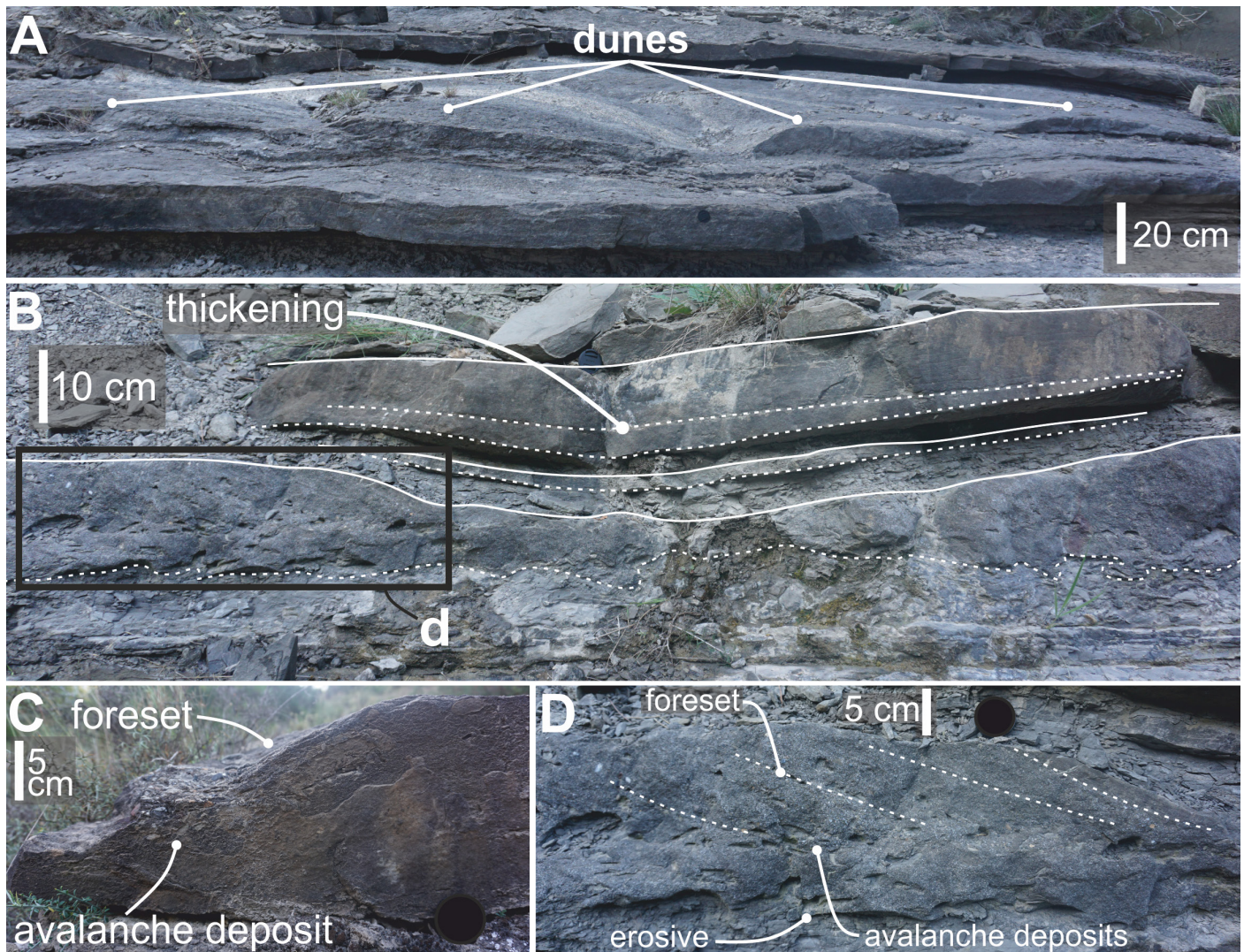


Figure 8 | (A) Dunes (label 2 on Figure 6A) developed above more structureless division. (B) Thickening of overlying beds into relief developed between dunes. (C) Dune foreset and grain flow deposit formed via ‘avalanching’ down lee-slope. Grain flow deposits are composed of lithic and mud clasts. (D) Zoomed view of B showing cross-stratification and grain flow deposits above more structureless and erosive division with mud clasts.

thick mud caps are observed (Remacha & Fernández, 2003; Bell et al., 2018).

These observations and interpretations are consistent with direct measurements of present-day turbidity currents, which indicate that they are driven by a high-velocity thin and dense basal head that drives the migration of crescentic bedforms and knickpoints (Figure 10) (Aspiroz-Zabala et al., 2017; Paull et al., 2018; Normandeau et al., 2020; Heijnen et al., 2020; Chen et al., 2021; Pope et al., 2022; Talling et al., 2022). The dense basal layer is followed by a more dilute body that slows as it thickens over hours to days (Aspiroz-Zabala et al., 2017; Pope et al., 2022). A similar flow structure is suggested to explain the dune-prone sandstone beds here, with the deposit of the dense basal layer reworked into dunes by the trailing body. Grain size and sorting variability within these dunes may reflect velocity fluctuations measured during the sustained passage of trailing flow bodies, as observed in turbidity currents of the Congo Canyon (Figure 10) (Aspiroz-Zabala et al., 2017; Talling et al., 2022).

5.2. Dunes or pseudo-dunes

As Arnott et al. (2017) noted, cross-stratification may form through turbidity current deposition within seabed scours (‘pseudo-dunes’), with the resulting deposit resembling dunes constructed above the seabed. Some of the cross-stratified beds discussed here display features similar to those observed in pseudo-dunes where they transition laterally to structureless sandstones, overlie structureless sandstones and have erosive bases. The reddish colour of the pseudo-dune beds of Arnott et al. (2017) and some of the beds described here are also comparable. Arnott et al. (2017) ascribed the colouration to early diagenesis and ferric-cementation due to relatively high depositional porosity and permeability. These beds have also been observed to be associated with scours elsewhere in the basin (Bakke et al., 2008). However, some of the sandstones in the studied package have positive seabed relief (Figures 6 and 7), indicating they were constructional and are, therefore, depositional bedforms.

It is possible that both pseudo-dune and dune formation occurred contemporaneously, as the high-magnitude flows

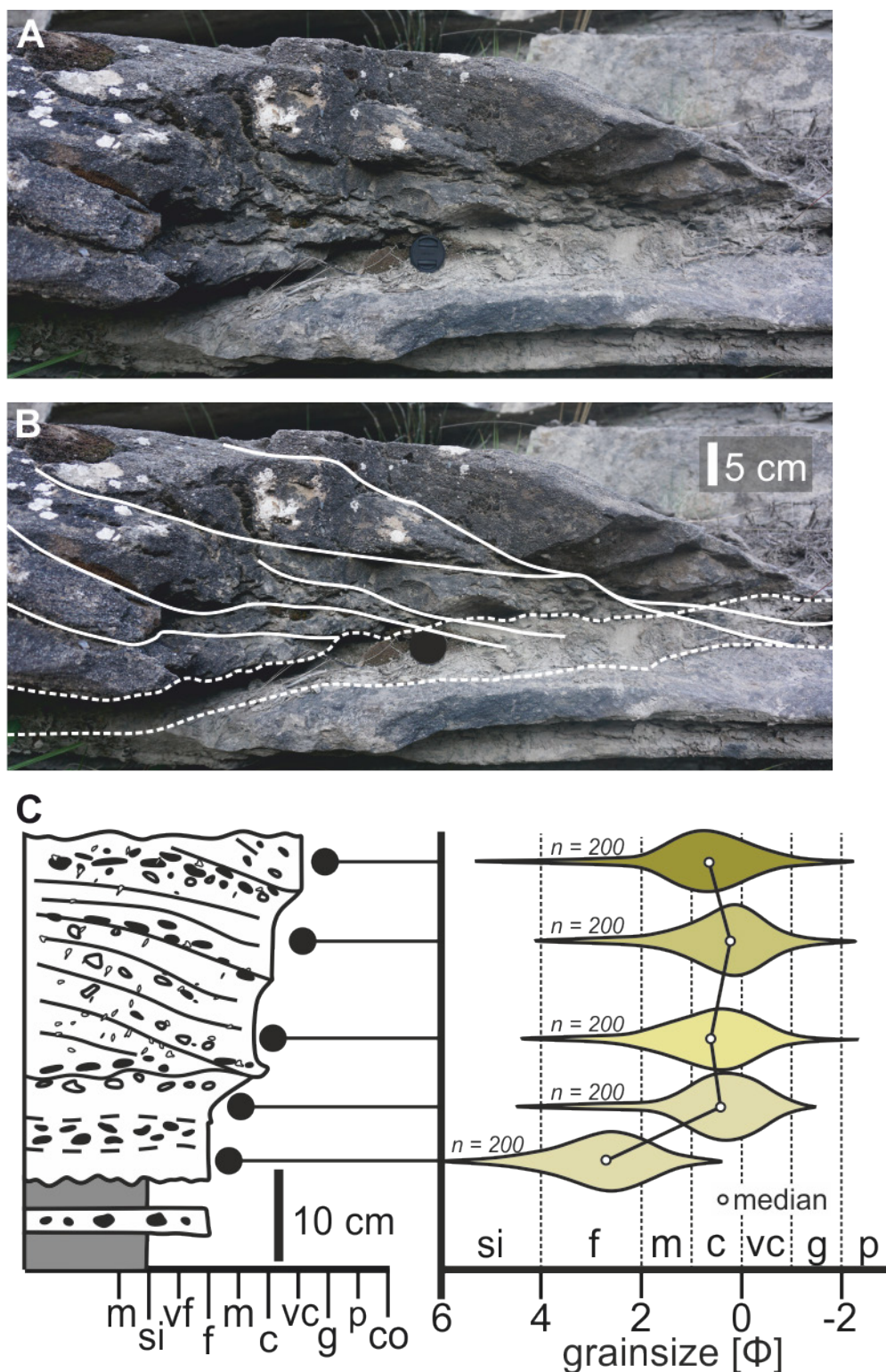


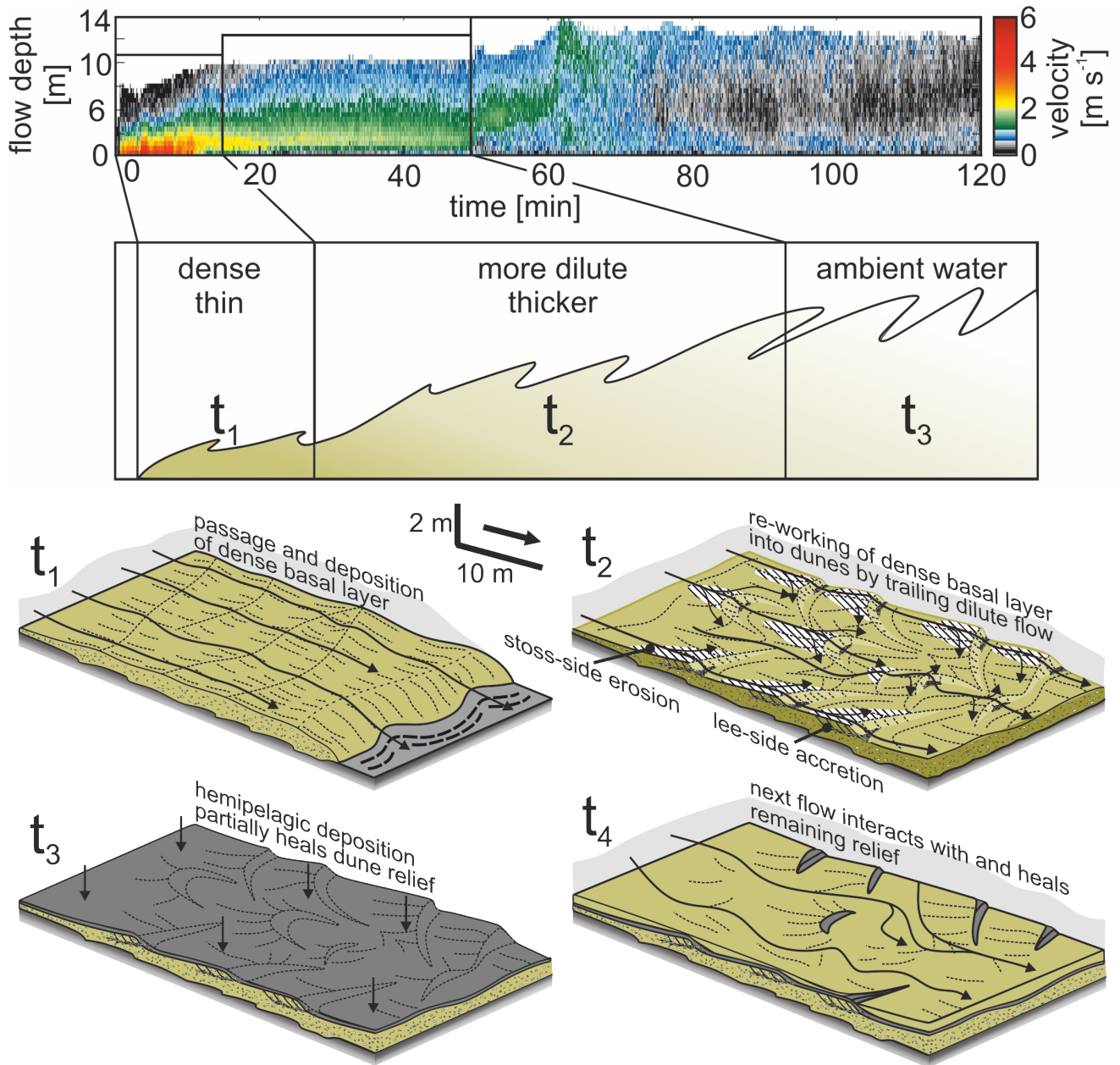
Figure 9 | (A) Sampled bed (Figure 5) and (B) detailed measured section. Violin plots show grain sizes measured via point-counting. The inversely-graded basal division passes upward into a cross-stratified coarse-grained division.

responsible for the deposition of these coarse-grained beds would have been capable of contemporaneous scouring and dune formation. The cross-stratification observed in some beds may therefore have been formed via scour-fill processes, while others are the product of dune-building. It is often difficult to differentiate between these owing to the scale of the outcrop compared to the potential scale of seabed scours (tens of metres to kilometres, see Hofstra et al., 2015, for compilation of scour dimensions) and the impacts of compaction after burial

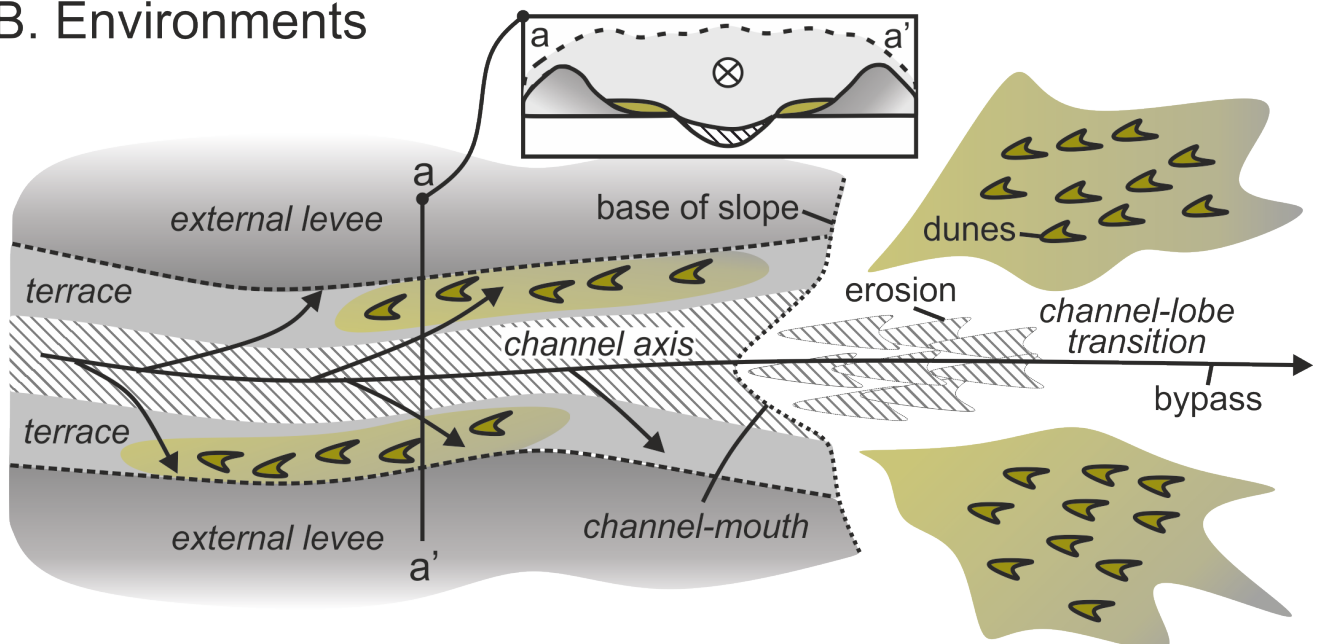
on deposits of varying grain size distorting primary depositional architectures.

On a lower resolution dataset, such as bathymetric data, these dune fields may be entirely unresolved within such large scours, or perhaps resemble upstream-migrating crescentic bedforms formed by transcritical (alternating between supercritical and subcritical) turbidity currents (e.g., Hage et al., 2018; Normandeau et al., 2020). In such cases the lee-slopes of the crescentic bedforms may be in fact aggrading and migrating downslope, and not being

A. Processes



B. Environments



↑ **Figure 10** | (A) Sedimentary process model for the development of the deposits identified in this study, based on a synthesis of turbidity current direct measurements (modified from Pope et al., 2022). The dense basal layer of the flow is interpreted to have deposited the initial coarse-grained deposit before reworking the deposit into dunes by the flow body. The dunes are formed by stoss-side erosion, and a combination of lee-side accretion, with spoon-shaped scours mantled with mud clasts forming on the lee-side of the dune. (B) Depositional environments in which dunes are most likely to be developed in deep-marine environments (channel environments from Hansen et al., 2017).

eroded and migrating upslope, with both processes resulting in similar seafloor morphologies. Time-lapse bathymetric surveys demonstrating migration direction are therefore essential when seeking to understand the characteristics of flows creating these features (Hage et al., 2018; Normandeau et al., 2020).

5.3. Depositional environments

These beds occur within successions dominated by thin-bedded and fine-grained turbidites and mass-transport deposits, and are interpreted to represent proximal overbank deposits confined by an unstable lateral basin margin (Figure 2) (Martínez-Doñate et al., 2023). This is analogous to the confinement felt by periodic, high-magnitude turbidity currents that fill entire channel belts and are therefore confined (and sustained) by levee walls. Elsewhere in the depocentre, dune-prone units similar to those described here have been identified beneath coarse-grained channel-fills (Tek et al., 2020), lateral to channels (Bakke et al., 2008; Cornard & Pickering, 2019; Tek et al., 2020), and immediately upstream of fine-grained basinal mudstones (Mutti & Normark, 1987; Mutti, 1991), supporting the interpretation that these beds are the depositional remnants of flows that bypassed sediment at channel mouth transition zones (Hodgson et al., 2022) and across the channel overbank areas (Mutti & Normark, 1987; Mutti, 1991) (Figures 10 and 11). Similar deep-marine dune or cross-stratified facies have been attributed to sediment bypass and reworking of the seabed by high-magnitude flows in the Cretaceous Lysing Formation, offshore Norway (Hansen et al., 2021), bottomsets of Miocene clinothems, offshore New Jersey (Stevenson et al., 2015; Hodgson et al., 2018), in the Eocene-Oligocene Grès d'Annot of France (Amy et al., 2000) and the Ranzono Sandstone of the Italy (Tinterri et al., 2017) deposited in Alpine orogeny foreland and piggyback basins.

The presence of coarse-grained deposits lateral to channels indicates the parent flows were of a sufficiently high velocity to escape the channel thalweg confinement without filtering out the coarse-grained fraction, suggesting that these deposits are representative of flows bypassing through the channel axis (Figure 10) (e.g., McArthur et al., 2020). This is also supported by abundant *Thalassinoides* burrows on bed tops, which suggest high energy, and therefore axial, environments (Heard & Pickering, 2008). These bedform-rich packages, therefore, provide an insight into the flows that cut the channels but that left little or no depositional trace within the channel thalweg itself (Englert et al., 2020). The poor preservation potential of these packages, coupled with the rare hydrodynamic conditions required for dune formation

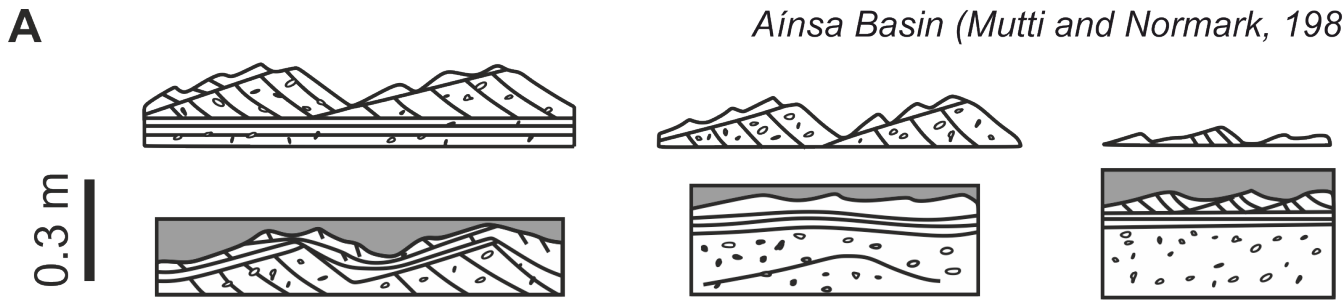
within turbidity currents (e.g., Arnott, 2012, Tilston et al., 2015), may be the reason for the lack of dunes in ancient deep-water successions, as dune-bearing packages will be frequently cannibalised by avulsion or propagation of their associated channels (e.g., Hodgson et al., 2022); or simply not being recognised at outcrop due to their relatively low thicknesses and affinity with weathered fine-grained sediments. Differentiation between channel overbank versus channel mouth could be supported by the characteristics of the surrounding stratigraphy. If the stratigraphy is predominantly fine-grained and heavily scoured then a channel mouth setting may be favoured, while a sandier surrounding stratigraphy composed of more variable grain sizes and bed thickness may favour an overbank interpretation. Differentiation could also be achieved where exposure or seismic resolution allows for lateral correlation toward a channel, or up-dip correlation toward a channel mouth.

While it is difficult to quantify whether these bedforms are better preserved in the Aínsa Basin compared to other basins owing to exposure bias, the preservation potential of these deposits in the Aínsa Basin may have been favoured by enhanced lateral migration of channels adjacent to the deforming thrust front (e.g., Bayliss & Pickering, 2015), resulting in channel mouths and overbanks being quickly abandoned and not cannibalised (Hodgson et al., 2022), high aggradation rates (Pemberton et al., 2016; Hodgson et al., 2022), early cementation aided by intense bioturbation and high bioclastic (and hence carbonate) content, or a combination of these factors.

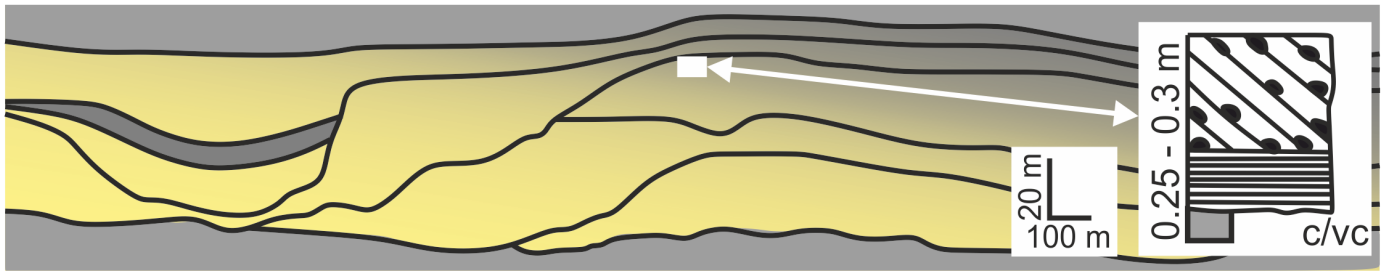
6. Conclusion

Sedimentary bedforms are formed by fluids of particular properties and aid palaeo-hydrodynamic reconstructions. One of the rarest depositional bedforms found in exhumed deep-marine environments are dunes, resulting in the conditions required for their formation and preservation being uncertain when compared with other bedforms. Here, using Eocene deep-marine strata of the Aínsa Basin, Spain, we document the sedimentology of an extremely well-exposed package of three-dimensional coarse-grained dunes, which allows for the internal structure and palaeoenvironmental significance of these bedforms to be investigated. The dune-bearing beds are composed of an inversely-graded, structureless division overlain by down-stream migrating dunes and scours, with superimposed fine-grained ripples formed on the dune stoss-sides. Following published direct measurements of turbidity currents, we interpret these dunes as having formed beneath the sustained body of high-magnitude turbidity currents, with the structureless division beneath

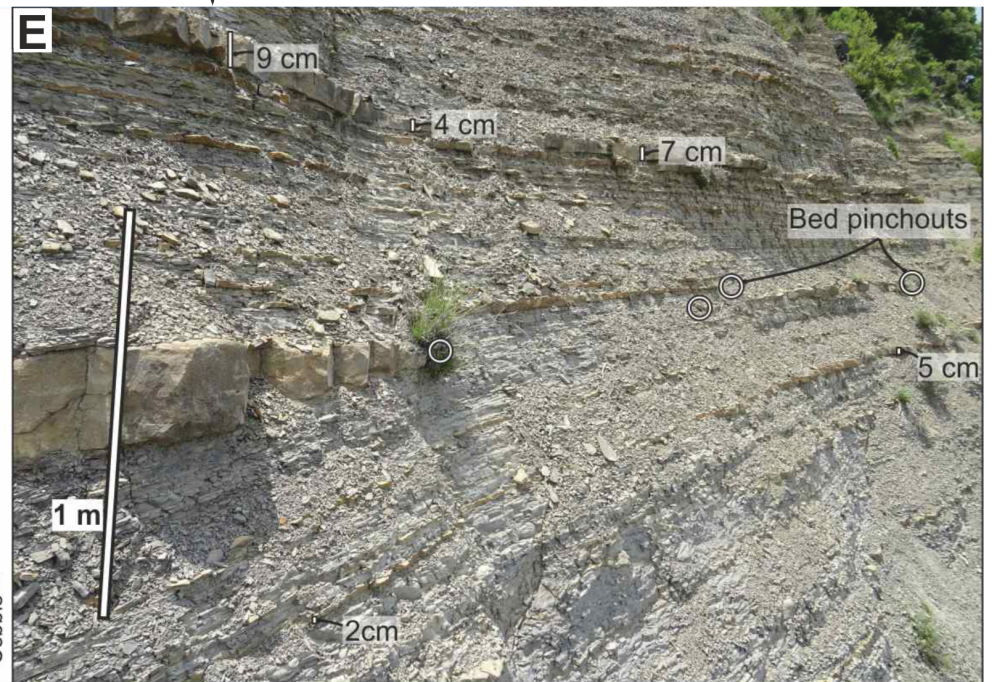
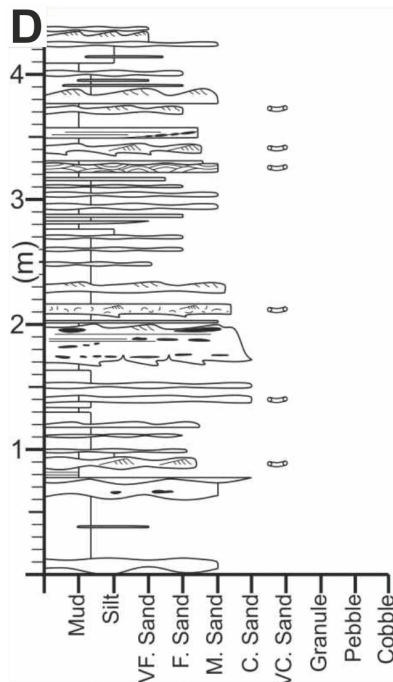
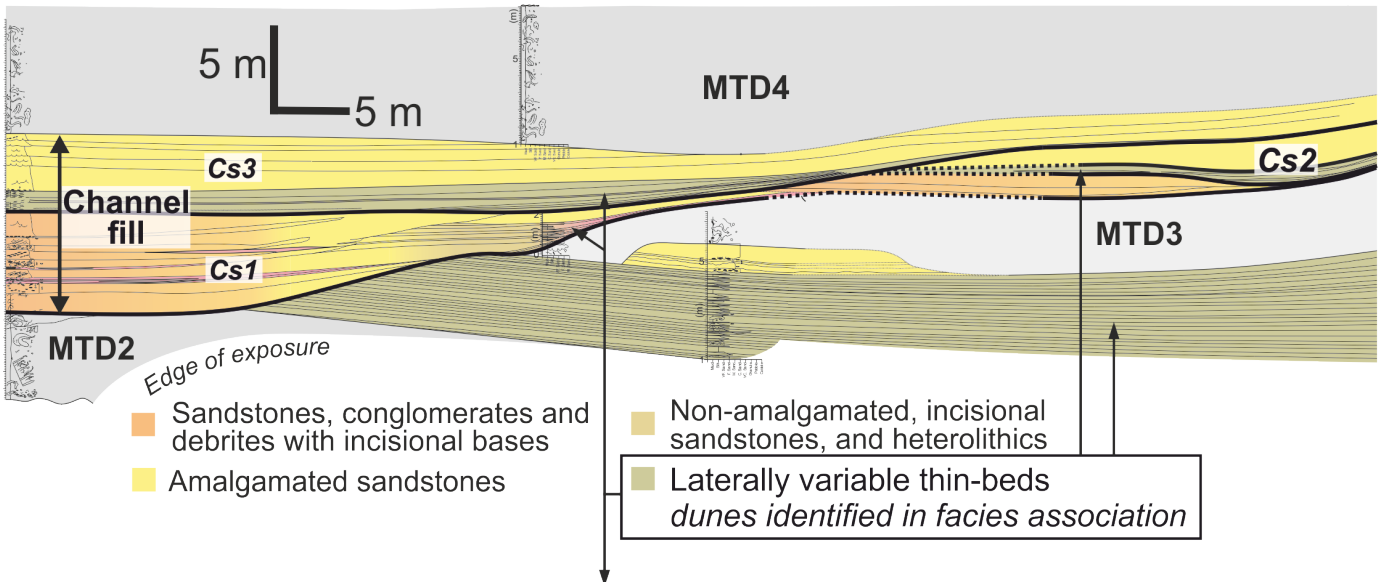
Aínsa Basin (Mutti and Normark, 1987)



Aínsa System, Aínsa Basin (Bakke et al. 2011)



Arro System, Aínsa Basin (Tek et al. 2020)



↑ **Figure 11** | Examples of similar facies observed in other studies in the Aínsa Basin. (A) Sketches of these facies across the Aínsa Basin (Mutti & Normark, 1987). (B) Modified outcrop sketch of the Aínsa system used as a basis for a seismic model by Bakke et al. (2008) and the location of dune-like facies reported from their facies table. (C) Correlation panel of an Arro system channel complex in the Aínsa Basin (modified from Tek et al. (2020)). Dunes have been reported from the 'laterally variable thin beds' facies association by Tek et al. (2020). Cs; channel system, MTD; mass-transport deposit. Measured section (D) and image (E) of the dune-prone laterally-variable thin beds (modified from Tek et al., 2020). Note facies similarities with Figures 3, 4 and 5.

the dunes representing the dense basal head of the current that was subsequently reworked. Scouring of dune stoss-sides during downstream migration and the development of superimposed ripples during flow waning modified the preserved dune shape, resulting in curvilinear dune crests and spoon-shaped scours being preserved in planform.

These dunes are associated with channelised environments and are interpreted to have been formed by flows that bypassed the channel axis and became depositional upon expanding across the channel overbank or encountering local accommodation, such as a scour. Similar deposits have been identified elsewhere in the basin-fill, and interpreted to have been formed beneath high-magnitude flows that became similarly unconfined at the mouths of submarine channels or formed within scours. Where identified in the stratigraphic record, these dune-rich intervals may therefore represent the passage of high-magnitude turbidity currents and thus significant bypass into the deep-basin.

Acknowledgments

Cai Puigdefàbregas and Dan Tek are thanked for discussions on the Aínsa Basin and its dunes. Dan Tek is thanked for sharing his and co-authors' figures on the Arro system. Allard Martinius and Richard Wild are thanked for their detailed revisions, which improved the clarity of the manuscript. The authors thank the Slope project Phase 5 sponsors for financial support: BP, Aker BP, BHP, CNOOC, Hess, Murphy, Neptune Energy, Petrobras, Vår Energi, and Wintershall DEA.

Authors contribution

ES: Conceptualization, data collection, data analysis, data interpretation, manuscript original draft. AMD: Conceptualization, data collection, data interpretation, manuscript review & editing. IK: Conceptualization, data collection, data interpretation, manuscript review & editing. MPM: Conceptualization, data interpretation, manuscript review & editing. WT: Data collection, data interpretation, manuscript review & editing. DH: Data collection, data interpretation, manuscript review & editing. MB: Data interpretation, manuscript review & editing. SF: Data interpretation, manuscript review & editing.

Data availability

All dune measurements are available in the supplementary files.

Conflict of interest

The authors declare no conflict of interest.

References

- Allen, J. R. L. (1982). *Sedimentary structures, their character and physical basis*, vol. 1. Elsevier, 593 p.
- Amy, L.A., Kneller, B. & McCaffrey, W. (2000). Evaluating the links between turbidite characteristics and gross system architecture: upscaling insights from the turbidite sheet-system of Peira Cava, SE France. *Deep Water Reservoirs of the World*, 1-15. <https://doi.org/10.5724/gcs.00.15.0001>
- Arnott, R.W.C. (2012). Turbidites, and the case of the missing dunes. *Journal of Sedimentary Research*, 82(6), 379-384. <https://doi.org/10.2110/jsr.2012.29>
- Arnott, R.W.C. & Al-Mufti, O. (2017). Deep-Marine Pseudo Dune Cross-Stratification—Similar, But Completely Different. *Journal of Sedimentary Research*, 87(3), 312-323. <https://doi.org/10.2110/jsr.2017.21>
- Ashley, G.M. (1990). Classification of large-scale subaqueous bedforms; a new look at an old problem. *Journal of Sedimentary Research*, 60(1), 160-172. <https://doi.org/10.2110/jsr.60.160>
- Azpiroz-Zabala, M., Cartigny, M. J. B., Talling, P. J., Parsons, D. R., Sumner, E. J., Clare, M. A., Simmons, S. M., Cooper, C., & Pope, E. L. (2017). Newly recognized turbidity current structure can explain prolonged flushing of submarine canyons. *Science Advances*, 3(10), e1700200. <https://doi.org/10.1126/sciadv.1700200>
- Baas, J.H., & Best, J.L. (2002). Turbulence modulation in clay-rich sediment-laden flows and some implications for sediment deposition. *Journal of Sedimentary Research*, 72(3), 336-340. <https://doi.org/10.1306/120601720336>
- Baker, M.L. & Baas, J.H. (2020). Mixed sand-mud bedforms produced by transient turbulent flows in the fringe of submarine fans: Indicators of flow transformation. *Sedimentology*, 67(5), 2645-2671. <https://doi.org/10.1111/sed.12714>
- Bakke, K., Gjelberg, J. & Petersen, S.A. (2008). Compound seismic modelling of the Aínsa II turbidite system, Spain: Application to deep-water channel systems offshore Angola. *Marine and Petroleum Geology*, 25(10), 1058-1073. <https://doi.org/10.1016/j.marpetgeo.2007.10.009>
- Barnolas, A. & Teixell, A. (1994). Platform sedimentation and collapse in a carbonate-dominated margin of a foreland basin (Jaca basin, Eocene, southern Pyrenees). *Geology*, 22(12), 1107-1110. [https://doi.org/10.1130/0091-7613\(1994\)022<1107:PSACIA>2.3.CO;2](https://doi.org/10.1130/0091-7613(1994)022<1107:PSACIA>2.3.CO;2)
- Bayliss, N. & Pickering, K.T., (2015). Transition from deep-marine lower-slope erosional channels to proximal basin-floor stacked channel-levée-overbank deposits, and syn-sedimentary growth structures, Middle Eocene Banastón System, Aínsa Basin, Spanish Pyrenees. *Earth-Science Reviews*, 144, 23-46. <https://doi.org/10.1016/j.earscirev.2014.11.015>
- Bell, D., Stevenson, C.J., Kane, I.A., Hodgson, D.M. & Poyatos-Moré, M. (2018). Topographic controls on the development

- of contemporaneous but contrasting basin-floor depositional architectures. *Journal of Sedimentary Research*, 88(10), 1166-1189. <https://doi.org/10.2110/jsr.2018.58>
- Blair, T.C. & McPherson, J.G. (1999). Grain-size and textural classification of coarse sedimentary particles. *Journal of Sedimentary Research*, 69(1), 6-19. <https://doi.org/10.2110/jsr.69.6>
- Bouma, A.H. (1962). *Sedimentology of Some Flysch Deposits: A Graphic Approach to Facies Interpretation*. Elsevier, Amsterdam, 168 p.
- Boulesteix, K., Poyatos-Moré, M., Flint, S.S., Taylor, K.G., Hodgson, D.M. & Hasiotis, S.T. (2019). Transport and deposition of mud in deep-water environments: Processes and stratigraphic implications. *Sedimentology*, 66(7), 2894-2925. <https://doi.org/10.1111/sed.12614>
- Caja, M.A., Marfil, R., Garcia, D., Remacha, E., Morad, S., Mansurbeg, H., Amorosi, A., Martínez-Calvo, C. & Lahoz-Beltrá, R. (2010). Provenance of siliciclastic and hybrid turbidite arenites of the Eocene Hecho Group, Spanish Pyrenees: implications for the tectonic evolution of a foreland basin. *Basin Research*, 22(2), p. 157-180. <https://doi.org/10.1111/j.1365-2117.2009.00405.x>
- Cantalejo, B., Pickering, K.T., Miller, K.G. & Mac Niocaill, C. (2021a). Chasing the 400 kyr pacing of deep-marine sandy submarine fans: Middle Eocene Aínsa Basin, Spanish Pyrenees. *Journal of the Geological Society*, 178. <https://doi.org/10.1144/jgs2019-173>
- Cantalejo, B., Pickering, K.T., McNiocaill, C., Bown, P., Johansen, K. & Grant, M. (2021b). A revised age-model for the Eocene deep-marine siliciclastic systems, Aínsa Basin, Spanish Pyrenees. *Journal of the Geological Society*, 178(1). <https://doi.org/10.1144/jgs2019-131>
- Cartigny, M.J. & Postma, G. (2017). Turbidity current bedforms, in *Atlas of bedforms in the Western Mediterranean*: Springer, Cham. 29-33. https://doi.org/10.1007/978-3-319-33940-5_6
- Castelltort, S., Honegger, L., Adatte, T., Clark, J.D., Puigdefàbregas, C., Spangenberg, J.E., Dykstra, M.L. & Fildani, A. (2017). Detecting eustatic and tectonic signals with carbon isotopes in deep-marine strata, Eocene Aínsa Basin, Spanish Pyrenees. *Geology*, 45(8), 707-710. <https://doi.org/10.1130/G39068.1>
- Chen, Y., Parsons, D.R., Simmons, S.M., Williams, R., Cartigny, M.J., Hughes Clarke, J.E., Stacey, C.D., Hage, S., Talling, P.J., Azpiroz-Zabala, M. & Clare, M.A. (2021). Knickpoints and crescentic bedform interactions in submarine channels. *Sedimentology*, 68(4), 1358-1377. <https://doi.org/10.1111/sed.12886>
- Cisneros, J., Best, J., van Dijk, T., de Almeida, R.P., Amsler, M., Boldt, J., Freitas, B., Galeazzi, C., Huizinga, R., Ianniruberto, M. & Ma, H. (2020). Dunes in the world's big rivers are characterised by low-angle lee-side slopes and a complex shape. *Nature Geoscience*, 13(2), 156-162. <https://doi.org/10.1038/s41561-019-0511-7>
- Collinson, J., & Mountney, N. (2019). *Sedimentary Structures 4th Edition*. Dunedin Academic Press, 352 p.
- Conway, K.W., Barrie, J.V., Picard, K. & Bornhold, B.D. (2012). Submarine channel evolution: active channels in fjords, British Columbia, Canada. *Geo-Marine Letters*, 32(4), 301-312. <https://doi.org/10.1007/s00367-012-0280-4>
- Cornard, PH & Pickering, K.T. (2019). Supercritical-flow deposits and their distribution in a submarine channel system, middle Eocene, Aínsa Basin, Spanish Pyrenees. *Journal of Sedimentary Research*, 89(6), 576-597. <https://doi.org/10.2110/jsr.2019.34>
- Costello, W.R. & Southard, J.B. (1981). Flume experiments on lower-flow-regime bed forms in coarse sand. *Journal of Sedimentary Research*, 51(3), 849-864. <https://doi.org/10.1306/212F7DC4-2B24-11D7-8648000102C1865D>
- De Cala, I., Ohata, K., Dorrell, R., Naruse, H., Patacci, M., Amy, L.A., Simmons, S., McLelland, S.J. & McCaffrey, W.D. (2020). Relating the flow processes and bedforms of steady-state and waning density currents. *Frontiers in Earth Science*, 8, 535743. <https://doi.org/10.3389/feart.2020.535743>
- Dumas, S., Arnott, R.W.C. & Southard, J.B. (2005). Experiments on oscillatory-flow and combined-flow bed forms: implications for interpreting parts of the shallow-marine sedimentary record. *Journal of Sedimentary Research*, 75(3), 501-513. <https://doi.org/10.2110/jsr.2005.039>
- Englert, R.G., Hubbard, S.M., Matthews, W.A., Coutts, D.S. & Covault, J.A. (2020). The evolution of submarine slope-channel systems: Timing of incision, bypass, and aggradation in Late Cretaceous Nanaimo Group channel-system strata, British Columbia, Canada. *Geosphere*, 16(1), 281-296. <https://doi.org/10.1130/GES02091.1>
- Fedele, J.J., Hoyal, D.C., Barnaal, Z., Tulenko, J., Awalt, S. (2016). Bedforms created by gravity flows. in Budd, D., Hajek, E., Purkis, S. (eds.), *Autogenic Dynamics and Self-Organization in Sedimentary Systems*. SEPM Special Publication, 106, 95 -121. <https://doi.org/10.2110/sepm.106>
- Fernández, O., Muñoz, J.A., Arbués, P. & Falivene, O. (2012). 3D structure and evolution of an oblique system of relaying folds: the Aínsa basin (Spanish Pyrenees). *Journal of the Geological Society*, 169(5), 545-559. <https://doi.org/10.1144/0016-76492011-068>
- Ge, Z., Nemeč, W., Vellinga, AJ & Gawthorpe, R.L. (2022). How is a turbidite actually deposited? *Science Advances*, 8(3), eabl9124. DOI: 10.1126/sciadv.abl9124
- Hage, S., Cartigny, M.J., Clare, M.A., Sumner, E.J., Vendettuoli, D., Clarke, J.E.H., Hubbard, S.M., Talling, P.J., Lintern, D.G., Stacey, C.D. & Englert, R.G. (2018). How to recognise crescentic bedforms formed by supercritical turbidity currents in the geologic record: Insights from active submarine channels. *Geology*, 46(6), 563-566. <https://doi.org/10.1130/G40095.1>
- Hand, BM. (1997). Inverse grading resulting from coarse-sediment transport lag. *Journal of Sedimentary Research*, 67(1), 124-129. <https://doi.org/10.1306/D426850E-2B26-11D7-8648000102C1865D>
- Hansen, L., Janocko, M., Kane, I. & Kneller, B. (2017). Submarine channel evolution, terrace development, and preservation of intra-channel thin-bedded turbidites: Mahin and Avon channels, offshore Nigeria. *Marine Geology*, 383, 146-167. <https://doi.org/10.1016/j.margeo.2016.11.011>
- Hansen, L.A.S., Hodgson, D.M., Pontén, A., Thrana, C. & Latre, A.O. (2021). Mixed axial and transverse deep-water systems: The Cretaceous post-rift Lysing Formation, offshore Norway. *Basin Research*, 33(4), 2229-2251. <https://doi.org/10.1111/bre.12555>
- Heard, T.G. & Pickering, K.T. (2008). Trace fossils as diagnostic indicators of deep-marine environments, Middle Eocene Aínsa-Jaca basin, Spanish Pyrenees. *Sedimentology*, 55(4), 809-844. <https://doi.org/10.1111/j.1365-3091.2007.00922.x>
- Heijnen, M.S., Clare, M.A., Cartigny, M.J., Talling, P.J., Hage, S., Lintern, D.G., Stacey, C., Parsons, D.R., Simmons, S.M., Chen, Y. & Sumner, E.J. (2020). Rapidly-migrating and internally-generated knickpoints can control submarine channel evolution. *Nature communications*, 11(1), 1-15. <https://doi.org/10.1038/s41467-020-16861-x>

- Hodgson, D.M., Peakall, J. & Maier, K.L. (2022). Submarine channel mouth settings: processes, geomorphology, and deposits. *Frontiers in Earth Science*, 10, 790320. <https://doi.org/10.3389/feart.2022.790320>
- Hodgson, D.M., Browning, J.V., Miller, K.G., Hesselbo, S.P., Poyatos-Moré, M., Mountain, G.S. & Proust, J.N. (2018). Sedimentology, stratigraphic context, and implications of Miocene intrashelf bottomset deposits, offshore New Jersey. *Geosphere*, 14(1), 95-114. <https://doi.org/10.1130/GES01530.1>
- Hofstra, M., Hodgson, D.M., Peakall, J. & Flint, S.S. (2015). Giant scour-fills in ancient channel-lobe transition zones: Formative processes and depositional architecture. *Sedimentary Geology*, 329, 98-114. <https://doi.org/10.1016/j.sedgeo.2015.09.004>
- Kenyon, N.H., Akhmetzhanov, A.M. & Twichell, D.C. (2002). Sand wave fields beneath the Loop Current, Gulf of Mexico: reworking of fan sands. *Marine Geology*, 192(1-3), 297-307. [https://doi.org/10.1016/S0025-3227\(02\)00560-1](https://doi.org/10.1016/S0025-3227(02)00560-1)
- Kneller, B.C. & McCaffrey, W.D. (2003). The interpretation of vertical sequences in turbidite beds: the influence of longitudinal flow structure. *Journal of Sedimentary Research*, 73, 706-713(5). <https://doi.org/10.1306/031103730706>
- Komar, P. D. (1991). The hydraulic interpretation of turbidites from their grain sizes and sedimentary structures. *Deep-Water Turbidite Systems*, 41-53.
- Kuenen, P.H. & Migliorini, C.I. (1950). Turbidity currents as a cause of graded bedding. *The Journal of Geology*, 58(2), 91-127. <https://doi.org/10.1086/625710>
- Läuchli, C., Garcés, M., Beamud, E., Valero, L., Honegger, L., Adatte, T., Spangenberg, J.E., Clark, J., Puigdefabregas, C., Fildani, A., de Kaenel, E., Hunger, T., Nowak, A., & Castellort, S. (2021). Magnetostratigraphy and stable isotope stratigraphy of the middle-Eocene succession of the Ainsa basin (Spain): New age constraints and implications for sediment delivery to the deep waters. *Marine and Petroleum Geology*, 132, 105182. <https://doi.org/10.1016/j.marpetgeo.2021.105182>
- LeRoux, J.P. (2003). Can Dispersive Pressure Cause Inverse Grading in Grain Flows? Discussion. *Journal of Sedimentary Research*, 73(2), 333-334. <https://doi.org/10.1306/043002730333>
- Leeder, M.R. (1983). On the interactions between turbulent flow, sediment transport and bedform mechanics in channelised flows. *Modern and ancient fluvial systems*, 3-18. <https://doi.org/10.1002/9781444303773.ch1>
- Lowe, D. R. (1982). Sediment gravity flows; II, Depositional models with special reference to the deposits of high-density turbidity currents. *Journal of sedimentary research*, 52(1), 279-297. <https://doi.org/10.1306/212F7F31-2B24-11D7-8648000102C1865D>
- Lowe, D.R. (1988). Suspended-load fallout rate as an independent variable in the analysis of current structures. *Sedimentology*, 35(5), 765-776. <https://doi.org/10.1111/j.1365-3091.1988.tb01250.x>
- Martínez-Doñate, A., Soutter E.L., Kane, I.A., Poyatos-More, M., Hodgson, D.M., Ayckbourne, A.J.M., Taylor, W.J., Bouwmeester, M.J., & Flint, S.S. (2023). Submarine crevasse lobes controlled by lateral slope failure in tectonically-active settings: an exhumed example from the Eocene Ainsa Basin, (Spain). *Sedimentologica*. <https://doi.org/10.57035/journals/sdk.2023.e11.1068>
- McArthur, A., Kane, I., Bozetti, G., Hansen, L. & Kneller, B.C. (2020). Supercritical flows overspilling from bypass-dominated submarine channels and the development of overbank bedforms. *The Depositional Record*, 6(1), 21-40. <https://doi.org/10.1002/dep2.78>
- Meiburg, E. & Kneller, B. (2010). Turbidity currents and their deposits. *Annual Review of Fluid Mechanics*, 42, 135-156. <https://doi.org/10.1146/annurev-fluid-121108-145618>
- Miramontes, E., Jorry, S.J., Jouet, G., Counts, J.W., Courgeon, S., Le Roy, P., Guerin, C. & Hernández-Molina, F.J. (2019). Deep-water dunes on drowned isolated carbonate terraces (Mozambique Channel, south-west Indian Ocean). *Sedimentology*, 66(4), 1222-1242. <https://doi.org/10.1111/sed.12572>
- Mochales, T., Barnolas, A., Pueyo, E.L., Serra-Kiel, J., Casas, A.M., Samsó, J.M., Ramajo, J. & Sanjuán, J. (2012). Chronostratigraphy of the Boltaña anticline and the Ainsa Basin (southern Pyrenees). *GSA Bulletin*, 124(7-8), 1229-1250. <https://doi.org/10.1130/B30418.1>
- Mulder, T., Migeon, S., Savoye, B. & Faugères, J.C. (2001). Inversely graded turbidite sequences in the deep Mediterranean: a record of deposits from flood-generated turbidity currents? *Geo-marine letters*, 21, 86-93. <https://doi.org/10.1007/s003670100071>
- Mutti, E. & Normark, W.R. (1987). Comparing examples of modern and ancient turbidite systems: problems and concepts, in *Marine Clastic Sedimentology*. Springer, Dordrecht, 1-38. https://doi.org/10.1007/978-94-009-3241-8_1
- Mutti, E. (1991). Distinctive thin-bedded turbidite facies and related depositional environments in the Eocene Hecho Group (South-central Pyrenees, Spain). *Sedimentology*, 24(1), 107-131. <https://doi.org/10.1002/9781444304473.ch14>
- Normandeau, A., Bourgault, D., Neumeier, U., Lajeunesse, P., St-Onge, G., Gostiaux, L. & Chavanne, C. (2020). Storm-induced turbidity currents on a sediment-starved shelf: insight from direct monitoring and repeat seabed mapping of upslope migrating bedforms. *Sedimentology*, 67(2), 1045-1068. <https://doi.org/10.1111/sed.12673>
- Paull, C.K., Talling, P.J., Maier, K.L., Parsons, D., Xu, J., Caress, D.W., Gwiazda, R., Lundsten, E.M., Anderson, K., Barry, J.P. & Chaffey, M. (2018). Powerful turbidity currents driven by dense basal layers. *Nature communications*, 9(1), 1-9. <https://doi.org/10.1038/s41467-018-06254-6>
- Pemberton, E.A., Hubbard, S.M., Fildani, A., Romans, B. & Stright, L. (2016). The stratigraphic expression of decreasing confinement along a deep-water sediment routing system: Outcrop example from southern Chile. *Geosphere*, 12(1), 114-134. <https://doi.org/10.1130/GES01233.1>
- Pickering, K.T. & Hiscott, R.N. (1991). Contained (reflected) turbidity currents from the Middle Ordovician Cloridorme Formation, Quebec, Canada: an alternative to the antidune hypothesis. *Sedimentology*, 32, 373-394. <https://doi.org/10.1002/9781444304473.ch6>
- Pickering, K.T. & Bayliss, N.J. (2009). Deconvolving tectono-climatic signals in deep-marine siliciclastics, Eocene Ainsa basin, Spanish Pyrenees: Seesaw tectonics versus eustasy. *Geology*, 37(3), 203-206. <https://doi.org/10.1130/G25261A.1>
- Pope, E.L., Cartigny, M.J., Clare, M.A., Talling, P.J., Lintern, D.G., Vellinga, A., Hage, S., Açikalin, S., Bailey, L., Chapplow, N. & Chen, Y. (2022). First source-to-sink monitoring shows dense head controls sediment flux and runoff in turbidity currents. *Science Advances*, 8(20), eabj3220. <https://doi.org/10.1126/sciadv.abj3220>
- Puigdefabregas, C., & Souquet, P. (1986). Tectono-sedimentary cycles and depositional sequences of the Mesozoic and Tertiary from the Pyrenees. *Tectonophysics*, 129(1-4), 173-203. [https://doi.org/10.1016/0040-1951\(86\)90251-9](https://doi.org/10.1016/0040-1951(86)90251-9)

- Reading, H.G. (2009). *Sedimentary environments: processes, facies and stratigraphy*. John Wiley & Sons. 688
- Remacha, E. & Fernández, L.P. (2003). High-resolution correlation patterns in the turbidite systems of the Hecho Group (South-Central Pyrenees, Spain). *Marine and Petroleum Geology*, 20(6-8), 711-726. <https://doi.org/10.1016/j.marpetgeo.2003.09.003>
- Ricci Lucchi, F. & Valmori, E. (1980). Basin-wide turbidites in a Miocene, over-supplied deep-sea plain: a geometrical analysis. *Sedimentology*, 27(3), 241-270. <https://doi.org/10.1111/j.1365-3091.1980.tb01177.x>
- Rodrigues, S., Hernández-Molina, F.J., Fonnesu, M., Miramontes, E., Rebesco, M. & Campbell, D.C. (2022). A new classification system for mixed (turbidite-contourite) depositional systems: Examples, conceptual models and diagnostic criteria for modern and ancient records. *Earth-Science Reviews*, 104030. <https://doi.org/10.1016/j.earscirev.2022.104030>
- Schindler, R.J., Parsons, D.R., Ye, L., Hope, J.A., Baas, J.H., Peakall, J., Manning, A.J., Aspden, R.J., Malarkey, J., Simmons, S. & Paterson, D.M. (2015). Sticky stuff: Redefining bedform prediction in modern and ancient environments. *Geology*, 43(5), 399-402. <https://doi.org/10.1130/G36262.1>
- Sequeiros, O.E., Spinewine, B., Beaubouef, R.T., Sun, T., Garcia, M.H. & Parker, G. (2010). Bedload transport and bed resistance associated with density and turbidity currents. *Sedimentology*, 57(6), 1463-1490. <https://doi.org/10.1111/j.1365-3091.2010.01152.x>
- Simons, D. B., Richardson, E.V., & Haushild, W.L. (1963). *Studies of Flow in Alluvial Channels, Some Effects of Fine Sediment on Flow Phenomena*. US Geological Survey Professional Paper, 1489, 46 p.
- Southard, J.B. & Boguchwal, L.A. (1990). Bed configuration in steady unidirectional water flows; Part 2, Synthesis of flume data. *Journal of Sedimentary Research*, 60(5), 658-679. <https://doi.org/10.1306/212F9241-2B24-11D7-8648000102C1865D>
- Soutter, E.L., Bell, D., Cumberpatch, Z.A., Ferguson, R.A., Spychala, Y.T., Kane, I.A. & Eggenhuisen, J.T. (2021). The influence of confining topography orientation on experimental turbidity currents and geological implications. *Frontiers in Earth Science*, 8, p.540633. <https://doi.org/10.3389/feart.2020.540633>
- Stevenson, C.J., Jackson, C.A.L., Hodgson, D.M., Hubbard, S.M. & Eggenhuisen, J.T. (2015). Deep-Water Sediment Bypass. *Journal of Sedimentary Research*, 85(9), 1058-1081. <https://doi.org/10.2110/jsr.2015.63>
- Sumner, E.J., Talling, P.J., Amy, L.A., Wynn, R.B., Stevenson, C.J. & Frenz, M. (2012). Facies architecture of individual basin-plain turbidites: Comparison with existing models and implications for flow processes. *Sedimentology*, 59(6), 1850-1887. <https://doi.org/10.1111/j.1365-3091.2012.01329.x>
- Sylvester, Z. & Lowe, D.R. (2004). Textural trends in turbidites and slurry beds from the Oligocene flysch of the East Carpathians, Romania. *Sedimentology*, 51(5), 945-972. <https://doi.org/10.1111/j.1365-3091.2004.00653.x>
- Talling, P.J., Baker, M.L., Pope, E.L., Ruffell, S.C., Jacinto, R.S., Heijnen, M.S., Hage, S., Simmons, S.M., Hasenhündl, M., Heerema, C.J. & McGhee, C. (2022). Longest sediment flows yet measured show how major rivers connect efficiently to deep sea. *Nature communications*, 13(1), 1-15. <https://doi.org/10.1038/s41467-022-31689-3>
- Tek, D.E., Poyatos-Moré, M., Patacci, M., McArthur, A.D., Colombera, L., Cullen, T.M. & McCaffrey, W.D. (2020). Syndepositional tectonics and mass-transport deposits control channelised, bathymetrically complex deep-water systems (Aínsa depocenter, Spain). *Journal of Sedimentary Research*, 90(7), 729-762. <https://doi.org/10.2110/jsr.2020.38>
- Tilston, M., Arnott, R.W., Rennie, C.D. & Long, B. (2015). The influence of grain size on the velocity and sediment concentration profiles and depositional record of turbidity currents. *Geology*, 43(9), 839-842. <https://doi.org/10.1130/G37069.1>
- Tinterri, R., Laporta, M. & Ogata, K. (2017). Asymmetrical cross-current turbidite facies tract in a structurally-confined mini-basin (Priabonian-Rupelian, Ranzano Sandstone, northern Apennines, Italy). *Sedimentary Geology*, 352, 63-87. <https://doi.org/10.1016/j.sedgeo.2016.12.005>
- Todd, B.J. (2005). Morphology and composition of submarine barchan dunes on the Scotian Shelf, Canadian Atlantic margin. *Geomorphology*, 67(3-4), 487-500. <https://doi.org/10.1016/j.geomorph.2004.11.016>
- Tsoar, H. (2001). Types of aeolian sand dunes and their formation. In: *Geomorphological fluid mechanics*. Springer, Berlin, Heidelberg, 403-429
- van Lunsen, H.A. (1970). *Geology of the Ara-Cinca region, Spanish Pyrenees, Province of Huesca*. Ph.D. Thesis, Utrecht State University, 119 p.
- Walker, R.G. (1965). The origin and significance of the internal sedimentary structures of turbidites. *Proceedings of the Yorkshire Geological Society*, 35(1), 1-32. <https://doi.org/10.1144/pygs.35.1.1>
- Walton, E.K. (1967). The sequence of internal structures in turbidites. *Scottish Journal of Geology*, 3(2), 306-317. <https://doi.org/10.1144/sjg0302030>
- Wynn, R.B., Masson, D.G. & Bett, B.J. (2002). Hydrodynamic significance of variable ripple morphology across deep-water barchan dunes in the Faroe-Shetland Channel. *Marine Geology*, 192(1-3), 309-319. [https://doi.org/10.1016/S0025-3227\(02\)00561-3](https://doi.org/10.1016/S0025-3227(02)00561-3)

How to cite: Soutter, E., Martínez-Doñate, A., Kane, I., Poyatos-Moré, M., Taylor, W., Hodgson, D. M., Bouwmeester, M. J., & Flint, S. (2024). Exceptional preservation of three-dimensional dunes on an ancient deep-marine seafloor: implications for sedimentary processes and depositional environments. *Sedimentologica*, 2(1), 1-18. <https://doi.org/10.57035/journals/sdk.2024.e21.1067>

